8-2015

Improved oncolytic virotherapy by increasing virus spread within tumors.

Stephen Wechman
University of Louisville

IMPROVED ONCOLYTIC VIROTHERAPY BY INCREASING VIRUS SPREAD WITHIN TUMORS

By

Stephen Wechman
B.S., Georgetown College, 2011

A Thesis

Submitted to the Graduate Faculty of the
University of Louisville School of Medicine
in Partial Fulfillment of the Requirements
for the degree of

Master of Science
in Pharmacology and Toxicology

Department of Pharmacology and Toxicology
University of Louisville
Louisville, Kentucky

August 2015

IMPROVED ONCOLYTIC VIROTHERAPY BY INCREASING VIRUS SPREAD WITHIN TUMORS

By

Stephen Wechman
B.S., Georgetown College, 2011

A Thesis Approved on

December 17, 2014

by the following Thesis Committee:

_____
Kelly M. McMasters, M.D., Ph.D.

_____
Heshan Zhou, Ph.D.

_____
J. Christopher States, Ph.D.

_____
Steven R. Myers, Ph.D.

_____
Kenneth E. Palmer, Ph.D.

DEDICATION

I dedicate this thesis to my beloved wife,

Sarah Wechman,

for her love and support during our 4 years together.

ACKNOWLEDGEMENTS

I would like to acknowledge Dr. Timothy Griffith for his quality instruction and for providing me the opportunity to research as an undergraduate student. I am very thankful to Dr. Kelly McMasters and Dr. Heshan Sam Zhou for allowing me to work in their laboratory and providing their expertise. I would also like to thank Dr. Shesh Nath Rai for his guidance and training as I performed the statistical analyses contained within this thesis. Lastly, I would like to thank Drs. Kelly McMasters, H. Sam Zhou, J. Christopher States, Steven Myers, and Kenneth Palmer for serving on my graduate committee.

ABSTRACT

IMPROVED ONCOLYTIC VIROTHERAPY BY INCREASING VIRUS SPREAD WITHIN TUMORS

Stephen Wechman

December 17, 2014

Oncolytic adenoviruses (Ads) have great therapeutic potential for lung cancer. Cancer selective *E1b*-deleted Ads are safe, however their efficacy remains limited clinically. To improve *E1b*-deleted Ads, Adhz60 was selected for greater anti-cancer efficacy by a process called bioselection, producing AdUV. AdUV preferentially lysed A549 and H1299 lung cancer cells more effectively than both the cancer selective Adhz60 and non-selective Ad5. AdUV induced greater LC3-II expression, relative to LC3-I, indicating that AdUV (30.9-fold) induced autophagy more effectively than Ad5 (12.2-fold) and Adhz60 (7.8-fold) in A549 cells. Mice treated with AdUV had significantly smaller tumors (p-value < 0.001) and prolonged survival (p-value = 0.0005) than mice treated with the negative control AdGFP. These results suggest that AdUV efficiently lyses lung cancer cells *in vitro* and *in vivo*.

TABLE OF CONTENTS

PAGE

LIST OF FIGURES

PAGE

CHAPTER I

INTRODUCTION

The leading cause of death from cancer is lung cancer. The number of lung cancer deaths (159,260) in 2014 was comparable to the number of deaths (159,810) from the next four leading cancers combined: colon, breast, pancreatic, and prostate (American Cancer Society). The Surveillance Epidemiology and End Results (SEER) statistics indicate that the five-year survival rate of lung cancer patients improved from 11.4% in 1975 to 17.5% in 2006. Lung cancer will continue to be a leading cause of death unless more effective treatments are developed.

Surgery is the best treatment option for early stage lung cancer. Lung cancer is staged using the Tumor Nodes Metastasis (TNM) system. Using this system, each patient is staged based upon the size of his/her primary tumor, lymph node involvement, and the presence or absence of distant metastasis [1]. Stage I lung tumors are less than 3 cm while stage II lung tumors are less than 7 cm in size [1]. Neither stage I nor stage II lung tumors have invaded tissue beyond their primary site, therefore lobe resection is feasible for most stage I and stage II lung cancer patients [2]. When lung cancer is surgically resected, 85% of stage I and 77% of stage II cancer patients survive at least two years after treatment [3]. Surgically resected stage II lung cancer is also frequently treated

with adjuvant platinum-based chemotherapeutics [4]. Therefore, surgery remains the best treatment option for early stage lung cancer.

For lung cancer patients beyond stage II, the combination of surgery, intravenous (IV) chemotherapy and radiation offer the best results clinically [5-7]. Stage III lung tumors are greater than 7 cm in size and have invaded one of the surrounding lung tissues such as the chest wall, pleura, or main bronchus [1]. Stage IV lung tumors can be of any size, however distant metastasis must be observed [1]. These distant metastases are frequently observed in the adrenal glands, bone, the opposite lung, liver or brain [8, 9]. The majority (57%) of lung cancer patients have distant metastases at the time of diagnosis. Therefore, most lung cancer patients are ineligible for surgery. Cancer chemotherapy has not significantly improved lung cancer patient survival despite the investigation of several different chemotherapeutic combinations clinically [10-12]. To treat lung cancer patients more effectively, novel cancer therapeutics and strategies are necessary.

The use of cancer selective viruses or oncolytic virotherapy is an emerging lung cancer treatment [13, 14]. Oncolytic adenovirus (Ad) therapy is unique because Ads can spread within tumors following the initial infection of a small number of cancer cells [13, 15]. Cancer selective Ads are generated by the attenuation of viral genes such as by the deletion of *E1b-19K* and *E1b-55K* [16-18]. ONYX-015 (*dl1520*) was the first cancer selective, *E1b-55k* deleted Ad studied clinically [19-21]. Many clinical trials studying *E1b*-deleted Ads have

recruited head and neck cancer patients as these tumors are accessible for intratumoral injection (IT). *E1b*-deleted Ads such as *dl1520* displayed favorable characteristics during several preclinical and clinical studies [20-22]. A virus very similar to *dl1520*, H101, was approved commercially in China for cancer therapy in combination with the PF chemotherapy regimen (cisplatin and fluorouracil) by the China Food and Drug Administration (CFDA) [23]. In a phase III trial, H101 treatment increased the tumor response rate in head and neck cancer patients treated with the PF regimen from 39.6% to 78.8% [24].

Ads are especially promising for the treatment of lung cancer. Ads have respiratory tropism, allowing them to very efficiently infect and therapeutically spread throughout the lung [25]. As a proof of concept, *E1b*-deleted Ads were shown to efficiently kill primary lung tumor cultures isolated at 0.1 multiplicity of infection (MOI) *in vitro* [26]. In a phase II clinical trial, Nemunaitis et. al. administered *dl1520* intravenously (IV) at increasing doses to patients with metastatic lung cancer [27]. Their research revealed that *dl1520* could infect and replicate within lung cancer patients tumors following IV injection. No serious side-effects were observed following *dl1520* treatment [27]. Furthermore, Ads interact synergistically with cancer chemotherapy as shown in primary lung cancer tissue *in vitro* and lung cancer xenograft models *in vivo* [22, 26, 28]. Cheng et. al. and Chen et. al. also reported synergistic interactions when *E1b*-deleted Ads were combined with rapamycin or indol-3-carbinol respectively *in vitro* [28, 29]. These studies indicate that adenovirus therapy is safe and cooperates with many cancer chemotherapeutics.

Multiple clinical trials have shown that Ads are safe and cancer selective, however their efficacy must be improved [19, 21, 23, 30, 31]. Bioselection can generate viruses with greater anti-cancer activity [32-34]. Bioselection typically entails the infection of cancer cells with viruses treated with mutagenic agents and reinoculated within cancer cell cultures. In this case, Adhz60 was treated with UV-light prior to the infection of the Ad-resistant Soas-2 cancer cells to select for more effective, cancer therapeutic Ads. Using bioselection, viruses with enhanced anti-cancer efficacy can be isolated without requiring a complete understanding of their virus-host interactions [32, 35]. By UV-irradiating Adhz60 and reinoculation in Soas-2 Ad-resistant cancer cells, AdUV was isolated (Fig. 1). AdUV displayed greater anti-cancer efficacy than Adhz60 in all cancer cell lines tested. AdUV also induced autophagy more effectively than both Adhz60 and Ad5 in A549 cells. These results suggest that AdUV may be released from and spread between cancer cells very efficiently. In addition, AdUV significantly suppressed the growth of A549 xenograft tumors and prolonged the survival of athymic nu/nu mice. These studies have demonstrated the great therapeutic potential of AdUV as a lung cancer therapeutic.

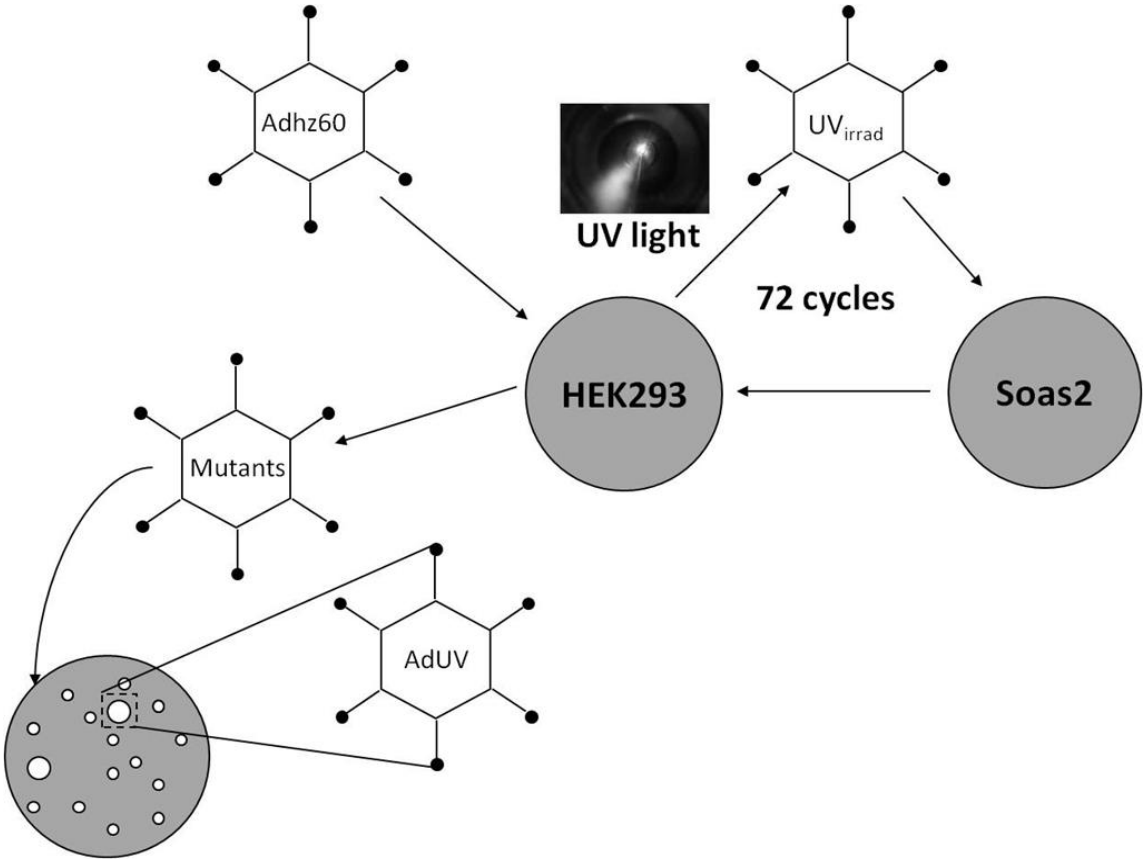

Figure 1. The bioselection process. Adhz60 was amplified in HEK293 cells prior to each cycle of UV-irradiation. Irradiated viruses (UV_{irrad}) then infected the Ad replication-resistant Soas-2 cancer cells. Viruses were harvested once cytopathic effects (CPE) were observed in Soas-2 cells. Viruses harvested from Soas-2 cells were then amplified in HEK293 cells before subsequent cycles of UV irradiation and bioselection. After 72 cycles of bioselection, AdUV was isolated by plaque purification from a large plaque formed upon Soas-2 cells. Adhz60 was treated with 639 J/m^2 UV type-C irradiation. UV-light was produced by a germicidal UV-lamp as described in the materials and methods.

CHAPTER II

MATERIALS AND METHODS

Cell lines and culture conditions

HEK293 (ATCC no. CRL-1573) human embryonic kidney, MRC5 (ATCC no. CCL171) normal lung fibroblast, A549 (ATCC no. CCL-185) human lung carcinoma, H1299 (ATCC no. CRL-5803) metastatic human lung carcinoma of the lymph node, H441 (ATCC no. HTB-174) lung papillary adenocarcinoma, and MCF7 (ATCC no. HTB-22) human breast adenocarcinoma cells were all purchased from the American Type Culture Collection (Rockville, MD). A549, MCF7, MRC5 and HEK293 cells were maintained in Dulbecco's Modified Eagle's medium (DMEM). H1299 and H441 cells were cultured in Roswell Park Memorial Institute (RPMI) 1640 medium. All cell culture media were supplemented with 10% fetal bovine serum, L-glutamine, and penicillin/streptomycin (100 U/mL). All cells were cultured and maintained in humidified 5% CO_2 incubators at 37^{o}C. All cell culture reagents were obtained from VWR (VWR, Radnor, PA).

Adenoviral vectors

Wildtype adenovirus serotype 5 (Ad5, ATCC no. VR-5) was used as a non-selective Ad control. Adhz60 has a deletion of the entire E1b gene and promoter and was used as a cancer selective Ad control [36]. AdGFP is an Ad

vector with the entire E1 gene (*E1a*, and *E1b*) deleted which expresses green fluorescent protein (GFP) driven by the CMV promoter. AdGFP does not replicate nor induce cytopathetic effects (CPE) in infected cells [28]. AdUV was generated by a process known as bioselection as illustrated in Figure 1. UV-light was used to irradiate Adhz60 for 5 minutes, inactivating approximately 90% of virus particles. UV-light was produced by a germicidal lamp, USEG30T3 (Sylvania, Danvers, MA), fitted with a 30 watt G30T8 UV-light bulb (Philips, Amsterdam, Netherlands) which produces UV type-C irradiation [37]. UV irradiation was measured with a model 25X UVX radiometer (Fisher Scientific, Waltham, MA). Using these conditions, 213 $\mu W/cm^2$ UV type-C was produced, generating a total UV dose of 639 J/m^2 after five minutes UV-irradiation (300 s). Irradiated viruses then used to infect Soas-2 cancer cells. Soas-2 cells do not support efficient Ad replication [38]. Ads were harvested from Soas-2 cells once CPE was observed. Harvested Ads were then amplified in HEK293 cells prior to subsequent UV-light irradiation. After 72 cycles of bioselection, viral clones were isolated by the plaque purification of large plaques formed on Soas-2 cells. The most active clone, AdUV, was used in this study. All Ad constructs are based on the Ad5 (wildtype) backbone sequence.

Viral infection and titration

Virus titer was determined using the infectious unit method as described previously [18, 39]. HEK293 cells were seeded overnight onto 96-well plates at a density of $1x10^3$ cells per well and infected with virus samples serially diluted

tenfold. The presence or absence of CPE in HEK293 cells was recorded after a minimum of 7 days incubation at 37^{o}C to calculate the virus titer or the number of virus particles per milliliter.

To determine the virus release kinetics, A549 cells were seeded into 12-well plates at a density of 1x10^{5} cells per well. Each well was infected with one MOI of Ad5, Adhz60 or AdUV. Samples were collected at 6, 24, 36, 48, and 72 hours post-infection. The cell culture media and cells were collected together. Virus infected cells were separated from the culture media by centrifugation using a micromax RF refrigerated microcentrifuge (Thermo Fisher Scientific, Waltham, MA) equipped with an IEC 851 rotor. Cells were centrifuged at 2,000 RPM (350 RCF), at 4^{o}C for five minutes. Media samples were then frozen at -80^{o}C, while cell pellets were resuspended in 1 mL of PBS and subjected to three freeze-thaw to release all virus particles into solution [28, 40]. Viral titers were then compared between Ad treatment groups by the number of virus particles inside (pellet) or outside (supernatant) of A549 cells.

Western blot analysis

A549 Cells were seeded at a density of 6x10^{5} per 60 mm dish and treated as indicated. Cells were collected and centrifuged at 1,500 RPM (453 RCF) at 4^{o}C for five minutes in an eppendorf 15 amp 5810 R refrigerated centrifuged equipped with a A-4-62 rotor (Eppendorf, Hamburg, Germany). The cell pellets were then washed with phosphate buffered saline (PBS) to remove serum contained within the cell culture media prior to cell lysis with Radio immuno

precipitation assay (RIPA) buffer containing 50 mM Tris-HCl, 150 mM NaCl, 1% NP-40, 0.5% sodium deoxycholate, and 0.1% sodium docecyl sulfate (SDS) with a protease inhibitor (PI) cocktail containing 4-(2-aminoethyl)-benzenesulfonyl fluoride (AEBSF), pepstatin A, L-trans-epoxysuccinyl-leucylamido(4-guanidino)butane (E-64), bestatin, leupeptin, and aprotinin (10 mL/10^6 cells; Sigma, St. Louis, MO). Cell pellets were incubated on ice in PI containing RIPA buffer for 30 minutes and homogenized every 10 minutes using a vortex-genie 2 to lyse cells (Scientific Industries, Bohemia, NY). Cell lysates were then centrifuged at 14,500 RPM (196,000 RCF) at 4^{o}C for 10 minutes to remove cell debris from the lysate using a Micromax RF microcentrifuge equipped with an IEC 851 rotor (Thermo Fisher Scientific, Waltham, MA). The cell pellets were discarded while the supernatant was stored for further experimentation. The protein concentration of all lysates was determined using the Pierce BCA protein assay kit according to the manufacturer's instructions (Thermo Fisher Scientific, Walton, MA). Equal amounts of cellular protein were resolved by electrophoresis through either 8% (E1A, hexon, penton, protein V, protein VI, protein VII) or 12% (LC3-I and LC3-II) SDS-polyacrylamide gels prior to transfer to Hybond-PVDF membranes activated with methanol (GE healthcare, Little Chalfont, UK) using a semi-dry transfer apparatus (BIO-RAD, Hercules, CA). Membranes were then blocked using 5% nonfat milk prepared in Tris-Buffered saline with Tween 20 (TBST) for one hour at room temperature. To detect protein expression, membranes were incubated with the following primary antibodies: rabbit-anti-adenovirus type 5 polyclonal antibody (1:10,000; abcam, Cambridge, England),

rabbit-anti-human LC3 monoclonal antibody (1:3,000; Novus Biologicals, Littleton, CO), rabbit-anti-human actin (1:2,000; Sigma, Saint Louis, MO) or mouse-anti-adenovirus E1A antibody (1:1,000; BD Pharmagen, San Jose, CA) at 4^{o}C on a lab-line thermal rocker overnight (Thermo Fisher Scientific, Waltham, MA). Primary antibody binding was detected by the incubation with the horse radish peroxidase (HRP) linked anti-mouse immunoglobin (Ig) or anti-rabbit Ig species-specific whole antibodies diluted 1:5,000 for one hour at room temperature (Amersham, Piscataway, NJ). All antibodies were diluted in TBST. Enhanced chemiluminescence (ECL) reagents were used to detect HRP-linked secondary antibody binding according to the manufacturer's instructions (Amersham, Piscataway, NJ). Light produced by the reaction of ECL and HRP was detected by exposure of membranes to CL-XPosure film 8 x 10 inches (Thermo Fisher Scientific, Waltham, MA) in an autoradiography cassette (Thermo Scientific, Pittsburgh, PA). Exposed films were then developed using a SRX-101A medical film processor according to the manufacturer instructions (Konica Minolta, Toyko, Japan). Developed films were then scanned using a Hewlett-Packard 4070 Scanjet scanner (Hewlett-Packard, Palo Alto, CA).

Plaque formation assay

A549 cells were seeded into 6-well plates at a density of 6x10^{5} per well. Cells were infected with Ad5, Adhz60 and AdUV at 0.01 MOI for 6 hours. The cell culture media were then removed and replaced with 5 mL of 1% nutrient agarose per well. The nutrient agarose was prepared by adding 1 g agarose (Fisher

Scientific, Waltham, MA) to 15 mL of double distilled water (ddH_20). This solution was then autoclaved in a Getinge model 533LS vacuum steam sterilizer on a LQ-15 cycle (Getinge, Lindholmen, Sweden). The agarose was then briefly reheated in a microwave on high for 30 to 45 seconds and mixed with 85 mL complete DMEM, the nutrient agarose medium was then equilibrated to approximately 44^oC prior to addition to cell monolayers. Images were taken six days post-infection with an EVOS FL microscope (Life technologies, Carlsbad, CA) at 4X magnification. The pixel densities of ten representative plaques per Ad5, Adhz60 and AdUV treatment groups were measured with the area density tool using Gel-pro analyzer 4.0 software according to the manufacturer's tutorial (Media cybernetics, Rockville, MD). The total number of pixels for each plaque was converted to millimeters (mm) by dividing the number of pixels per plaque by the number of pixels per one mm^2. The pixel length of one mm (510 pixels) was determined by the 1,000 micrometer (μm) scale bar to yield the pixels per one mm^2 of 260,100 pixels.

Quantification of band intensity

Band intensities were quantified by Gel-pro analyzer 4.0 software in accordance with the manufacturer's tutorial (Media Cybernetics, Bethesda, MD). Densitometric values were expressed as the integrated optical density (IOD) for each band. These data were reported as the ratio of LC3-II/LC3-I with each LC3-I and LC3-II band normalized to their respective to actin bands [28]. Mock treated cells were represented as one-fold LC3-II/LC3-I expression.

Cytotoxicity assay

Cells were seeded at a density of $2x10^4$ (H1299), $3x10^4$ (A549), $4x10^4$ (MCF-7) or $6x10^4$ (H441) cells per well onto 24-well plates. Cytotoxicity was assessed by crystal violet staining [41]. Suspended cells were removed by aspiration and the remaining adherent cells were fixed with 3.7% formaldehyde for 20 minutes at room temperature. Excess formaldehyde was washed away with PBS and cells were stained using 1% crystal violet at room temperature for 30 minutes. Excess crystal violet was washed away with water. Plates were then scanned using an HP Scanjet 4070 scanner (HP, Palo Alto, CA). The remaining crystal violet was then solubilized with a 2% sodium dodecyl sulfate (SDS) solution and the sample absorbances were measured at 590 nm using a Synergy HT Multi-Mode Microplate Reader (Bio-Tek, Winooski, VT). The absorbance (OD) values were then normalized to mock treated cells converting each sample OD into percent (%) cell viability by the formula, cell viability % = (OD of treated cells / OD of Mock treated cells) x 100%.

Lung cancer xenograft study

Tumors were formed by the subcutaneous injection (SC) of $5x10^6$ A549 lung cancer cells into the right flank of athymic nu/nu mice. Palpable tumors were observed two weeks following SC injection. Once tumors reached 30 mm^3, mice were randomized and treated by intratumoral injection (IT) with $5x10^8$ plaque forming units (PFU) of either AdGFP or AdUV. Tumor volumes were calculated based upon the following equation, $V = (L \times W^2)/2$, where L is length and W is the

width of the tumor [40]. Both Ad treatments were suspended in 50 µL prior to IT injection. Mice were injected four times with $5x10^8$ PFU of each treatment in three day intervals for a total dose of $2x10^9$ PFU. Eight mice were treated with AdGFP and seven mice were treated with AdUV. All animals were handled humanely and all experiments were conducted using an approved IACUC protocol.

DNA Sequencing

DNA sequencing was performed at the University of Louisville KBRIN bioinformatics core facility using Ion PGM Sequencing 200 kit v2 and Ion PGM system. One Ion 314 v2 Chip was used for loading the enriched Ion One Touch 200 ISP samples. Open source integrated genomics viewer (IGV) software was downloaded to view DNA sequence results. Mutations were considered to be present when the DNA was altered in greater than 95% of total reads for each gene region. Reading frames were observed using the translation track feature of IGV to determine if detected DNA mutations altered amino acid sequences.

Statistical analysis

All experiments were repeated at least three times. Quantification of results was reported as means of three independent experiments plus or minus (±) the standard deviation. The Pearson correlation coefficient (r) was used to evaluate the accuracy of equations used to calculate sample protein concentrations with the Pierce BCA protein assay kit. Statistical significance was assessed using analysis of variance analysis (ANOVA) and the Wilcoxon rank-

sum test. Multiple comparisons of ANOVA tests were corrected using Bonferroni's method. Multiple comparisons of Wilcoxon ranked-sum were corrected by Dunn's test. Adjusted p-values are reported for each of these multiple comparisons. These statistical tests cannot report adjusted p-values greater than 1.0 or less than 0.0001. All statistical tests were conducted using GraphPad software (Microsoft, Redmond, WA). Detailed methods for the analysis of each dataset are provided as follows.

Figures 3A-D were analyzed using two-way ANOVA to compare Adhz60 versus Ad5 and Adhz60 versus AdUV treatment groups. Multiple comparisons were made between each virus dose or MOI. The EC50 of each virus which lysed treated cancer cells (Ad5, Adhz60 and AdUV) was also determined. First, values were expressed as the percent death rather than percent viability the virus dose was logarithmically transformed by the equation ($x = \log(x)$). These data were then fit to their respective dose-response curves using log-agonist vs. normalized response regression analysis in Figure 3E. Considering AdUV had an EC50 of one MOI in A549 cells, a two-way ANOVA was used to observe if these data, Figure 3A-D, were significantly different at one MOI between all treatment groups and cell lines as tabulated in Figure 4F. Figures 4B and 5B were determined to have unequal variance between treatments groups by the Kruskal-Wallis test. Therefore, Figures 4B and 5B were analyzed using the Wilcoxon rank-sum test. Multiple comparisons were made using Dunn's test to determine if AdUV versus Ad5 and AdUV versus Adhz60 treatment groups were significantly different. Figure 8A was analyzed using two-way ANOVA to determine if tumor

growth following AdGFP and AdUV treatment was significantly different at each time-point (days). Figure 8C was analyzed using the Kaplan-Meijer Log-rank sum test to determine if the survival of mice following AdGFP and AdUV treatment was significantly different. These statistical tests were performed using GraphPad Prism software (Microsoft, Redmond, WA). Statistical significance was set at $p < 0.05$.

CHAPTER III

RESULTS

AdUV strongly destroys cancer cells.

AdUV was isolated by exposing Adhz60 to UV irradiation followed by selection in Ad-replication resistant Soas-2 cancer cells as illustrated in Figure 1. This process is called bioselection. The virus used for these studies, AdUV, was isolated from a large plaque formed on Soas-2 cells. The anti-cancer activity of AdUV was compared to the cancer non-selective wildtype Ad serotype 5 Ad5, the cancer selective *E1b*-deleted Ad Adhz60, and the *E1a*, *E1b*-deleted negative control Ad AdGFP. Ad5 and Adhz60 represent the positive and negative controls for MRC5 cell lysis respectively. H1299 human lung cancer and MRC5 normal lung cells were infected with AdGFP, Ad5, Adhz60, and AdUV at the indicated multiplicities of infection (MOI) for five days (Fig. 2A). AdUV induced greater cytopathic effect (CPE) than Adhz60 and Ad5 in H1299 lung cancer cells (Fig. 2A). AdUV also killed MRC5 normal cells more effectively than Adhz60, however less than Ad5 at 10 MOI (Fig. 2A). Therefore to test if AdUV was cancer selective, MRC5 normal and H1299 lung cancer cells were treated at MOI 10 and observed for CPE (Fig. 2B). Ad5 induced CPE non-selectively in both normal lung and lung cancer cells, while Adhz60 only induced CPE in H1299 lung cancer cells as expected. AdUV induced less CPE in MRC5 normal cells at 10 MOI than Ad5,

however AdUV induced more CPE in H1299 lung cancer cells than both Ad5 and Adhz60 (Fig. 2A, B).

To study the oncolytic effects of AdUV further, A549, H1299, and H411 lung cancer and MCF-7 breast cancer cells were treated with AdGFP, Ad5, Adhz60 or AdUV at the indicated MOIs for five days. The E1b-deleted Ad Adhz60 was applied as a cancer selective control [36]. Therefore, Ad5 and AdUV were compared to Adhz60 to determine if Ad5 or AdUV displayed greater anti-cancer efficacy than Adhz60. Cell viability was determined via crystal violet staining and normalized to mock (0 MOI) treated cells (Fig. 3). Ad5 very effectively induced cancer cell death in all four cancer cell lines tested, whereas AdGFP did not alter cell viability (Fig. 2A-D). AdUV killed A549 lung cancer cells more effectively than both Adhz60 (p-value = 0.0002) and Ad5 (p-value = 0.005) at 0.3 MOI (Fig. 3A). AdUV also killed H1299 lung cancer cells more effectively than Ad5 (p-value < 0.0001) and Adhz60 (p-value < 0.0001) at 0.3 MOI (Fig. 3B). Treatment with Ad5 at one MOI was more effective than Adhz60 in H411 lung (p-value < 0.0001) and MCF-7 breast (p-value = 0.0009) cancer cells respectively. Ad5 and AdUV treatments were not significantly different in H441 and MCF7 cells (Fig. 3C-D). Adhz60 was significantly less effective than both Ad5 and AdUV in all cancer cell lines (Fig. 3A-D).

The viability of AdUV treated A549 cells was lower than Ad5 and Adhz60 at all viral doses (MOI) tested. Therefore, studies investigated how AdUV killed A549 cells more effectively than Ad5. The EC50 values of Ad5, Adhz60 and

AdUV were determined for each cancer cell line (Fig. 3E). The EC50 of AdUV treated A549 cells was one MOI (0.99; Fig. 3E). Therefore, p-values were reported to determine if statistically significant differences were observed at one MOI between all Ads and cancer cell lines (Fig. 3F). These experiments taken together indicate that AdUV killed multiple cancer cell lines very efficiently with minimal effects upon MRC5 normal cells *in vitro*.

AdUV displays greater viral release from cells.

AdUV was selected for the efficient lysis of and release from cancer cells during bioselection. Therefore, the plaque assay was used to study AdUV spread through A549 lung cancer cells. AdUV formed larger plaques than Ad5 (p-value = 0.0248) and Adhz60 (p-value = 0.0002) in A549 cells (Fig. 4B). Larger plaque formation is indicative of more efficient cell lysis, release, and spread.

To study if the replication of AdUV was altered via bioselection, A549 cells were infected with Ad5, Adhz60 and AdUV at one MOI or the EC50 of AdUV (Fig. 3A, E). A549 cells infected with AdUV displayed greater E1A expression than Adhz60 treated cells at 24 hours post-infection (Fig. 5A). A similar pattern was observed at 72 hours as AdUV infected cells had greater late protein expression than Adhz60 treated cells. Ad gene expression was not detected in the mock treatment group.

The concentration of Ad particles in the cell culture media was studied to determine if AdUV was released more efficiently from A549 cells than Ad5 and

Adhz60 at one MOI, 48 hours post-infection. Adhz60 titer was 0.4-fold and AdUV titer was 0.7-fold relative to Ad5 within the cell fraction of infected A549 cells. AdUV titer was 3.3-fold in the cell-free fraction which was significantly greater than Adhz60 (p-value = 0.02) which was 0.1-fold relative to Ad5 (Fig. 5B). These data indicate that AdUV was released from A549 cells more efficiently than Adhz60 but not Ad5.

To study the release kinetics of AdUV across time, A549 cells were infected with Ad5, Adhz60 or AdUV at one MOI. Virus samples were collected from these infected cells at 6, 24, 48, and 72 hours post-infection. Ad5 and AdUV virus production was similar inside of A549 cells while Adhz60 virus titer was slightly attenuated (Fig. 5C, left). The titer of AdUV was greater in the cell culture media than both Ad5 and Adhz60 ($1.5x10^6$ of Ad5, $1.5x10^5$ of Adhz60, and $5x10^6$ of AdUV virus particles per ml at 48 hours) (Fig. 5C, right). AdUV was initially released from A549 cells at 36 hours post-infection (Fig. 5C, right). After 36 hours AdUV virus release plateaued (Fig. 5C, right). Therefore, increased AdUV release from A549 cells may contribute to the formation of larger plaques.

AdUV induces autophagy.

Autophagy was investigated to determine if increased autophagy induction could explain the enhanced release and oncolysis phenotypes of AdUV. Autophagy involves the lysosomal recycling of cytoplasmic organelles and long lived proteins [48]. It has been reported that autophagy enhances Ad replication perhaps by increasing cellular energy and nutrition for the assembly for virus

particles [42]. During autophagy, LC3-I is produced by the cleavage of pro-LC3 by the cysteine protease Atg4 into LC3-I [43, 44]. LC3-I matures into LC3-II by ATG3, ATG5, ATG7, and the ATG12-5 complex mediated conjugation of phosphatidylethanolamine (PE) to the LC3-I glycine amino acid [45]. Therefore, the LC3-II/LC3-I expression ratio was used to estimate autophagy induction and autophagosome abundance [45, 46]. While Ads are known to induce autophagy, it was necessary to confirm if AdUV induced LC3-II expression (Fig. 6A). AdUV treatment increased the LC3-II/LC3-I expression ratio by 2.0, 7.0, 9.1, and 13.6 fold in A549 cells infected at 0.1, 0.3, 1, and 3 MOIs respectively (Fig. 6A). Thus, LC3-II/LC3-I cleavage increased in a dose dependent manner with AdUV dose (MOI). Then, one MOI was selected to observe if autophagy induction varied between AdGFP, Ad5, Adhz60 and AdUV treatment groups five days post-infection. LC3-I conversion to LC3-II was detected in A549 cells treated with Ad5, Adhz60 and AdUV but not in the negative controls, mock or AdGFP, treatment groups (Fig. 6B). In this experiment, AdUV increased the LC3-II/LC3-I expression ratio 30.9 fold, greater than both Ad5 (12.2 fold) and Adhz60 (7.8 fold; Fig. 6B). A549 cells treated with one MOI of AdGFP, Ad5, Adhz60 or AdUV were photographed to observe changes in A549 cell morphology (400 x) three days post-infection. Cells treated with Ad5 and AdUV, but not AdGFP or Adhz60, displayed large cytoplasmic vesicles indicating autophagy activation morphologically at day three post-infection (Fig. 6C, arrowheads). These results indicate that AdUV induced autophagy more effectively than both Ad5 and Adhz60 in A549 cells.

Ion-torrent DNA sequencing of AdUV.

AdUV DNA was sequenced to identify mutations induced during bioselection [47]. Preliminary DNA sequencing revealed 31 mutations in the AdUV genome after sequence alignment to wildtype reference sequences (Fig. 7) [48]. Detailed analysis of mRNA open reading frames revealed that ten of these DNA mutations have altered at least one of their encoded amino acid residues (Fig. 7A). It is likely that some or all ten of these mutations are responsible for the oncolytic phenotype of AdUV (Fig. 7B). The mutation to *pIII* resulted in a non-sense mutation, truncating twelve amino acids 559 – 571. Ad5 *pIII* has not been studied, however studies of Ad serotype 2 (Ad2) indicate that pIII is highly phosphorylated relative to other peptides in the Ad2 proteome [49]. Lind et. al. predicted twelve phosphorylation sites were present in Ad2: one tyrosine, one threonine and ten serines. The Ad2 phosphorylation site (503 – 519) on the carboxy-terminus indicates that perhaps AdUV has lost a phosphorylation site at its carboxy-terminus. Ad5 and Ad2 pIII peptides are each 571 amino acids long and have 98.6% sequence identity. Another mutation to *Iva2* at position 4952 changed the encoded glycine to an alanine. Iva2 is associated with virus packaging, thus mutation of *Iva2* could lead to a possible mechanism of enhanced AdUV spread [50]. The mutation detected in *pV* at position 17387 changed a glycine to an arginine. Glycine is hydrophobic with a single hydrogen atom as a side chain, however arginine has a six carbon nitrogenous side-chain with a positive charge at physiological pH. The endogenous function of pV is to bind Ad DNA to the capsid by interaction with p32 [51]. Therefore, the

substitution of a neutral glycine for the positively charged (basic) arginine, may allow pV to bind the negatively charged DNA sugar-phosphate backbone more effectively. AdUV surprisingly is *E1b*-wildtype in addition to these mutations. AdUV may have regained *E1b* via the homologous recombination with the E1 region of HEK293 during bioselection [52]. These mutations likely increased the oncolytic efficacy of AdUV.

AdUV inhibits tumor growth in nude mice

DNA sequence analysis indicated that AdUV had regained the wildtype E1b gene, therefore the lethality and therapeutic efficacy of AdUV was tested in immunodeficient mice. The therapeutic effects of AdUV were evaluated using a human A549 lung cancer tumor xenograft nu/nu athymic mouse model. Once tumors reached 30 mm^3 in size mice were randomized into the AdGFP and AdUV treatment groups. Mice were injected intratumorally (IT) with 5×10^8 plaque forming units (PFU) of AdGFP or AdUV prepared in 50 microliters (μL) of phosphate-buffered saline (PBS). Four injections were administered to mice from day six every three days until day fifteen. AdGFP was used as a negative control for these studies. The length and width of each tumor was measured using calipers every three days until day 125. Tumor volumes were calculated based upon the following equation, $V = (L\times W^2)/2$, where L is length and W is the width of each tumor [40]. Mice were euthanized once tumor volumes exceeded 1,000 mm^3. The tumor sizes between AdGFP and AdUV treatment groups reached statistical significance at day thirty-three (p-value = 0.0363, Fig. 8A). AdUV

treated tumors were significantly smaller (93.8%) than AdGFP treated tumors at day 51 (p-value < 0.0001, Fig. 8A). Representative photographs of treated mice indicated that AdUV strongly inhibited A549 tumor growth compared to AdGFP at day fifty-one (Fig. 8B). All seven mice treated with AdUV survived until day 125 (p-value = 0.0005) while only two of eight total AdGFP treated mice survived (Fig. 8C). Thus, AdUV treatment significantly improved the survival of A549 tumor-bearing mice compared to the AdGFP treatment group. Of the seven mice treated with AdUV, two were tumor-free. The other five AdUV treated mice bore tumors which no longer grew but remained palpable until day 151. It is possible that AdUV was non-lethal in nude mice because human Ad replication is poor in murine relative to human cells. Therefore, AdUV may not be cancer selective *in vivo*. These results indicate that AdUV was safe and repressed A549 tumor growth in athymic nude mice.

CHAPTER IV

DISCUSSION

This study revealed the therapeutic potential of AdUV. AdUV was isolated following the UV-irradiation of the *E1b*-deleted Ad Adhz60 and selected in the Ad-resistant Soas-2 cancer cells during bioselection (Fig. 1) [36]. To my knowledge, this is the first time that bioselection has been used upon a cancer selective adenovirus (Ad). AdUV produced greater therapeutic effects than Adhz60 in all cancer cell lines tested. Focusing upon A549 lung cancer cells, the release of AdUV was greater than Adhz60 (p-value = 0.0204) but not Ad5 *in vitro* (Fig. 5B). The increased killing effects of AdUV may be related to greater autophagy induction in A549 cells (Fig. 6). Tumors treated with AdUV were significantly smaller than tumors treated with the negative control AdGFP (p-value < 0.0001; Fig. 8A). The overall survival of AdUV treated mice was significantly greater than AdGFP treated mice (p-value = 0.0005; Fig. 8C). These data indicate that AdUV is a promising lung cancer therapeutic agent with no observed lethality to immunodeficient mice *in vivo*.

Most of these mutations were located in the Ad structural genes. The absence of mutations to the early viral genes, such as E1 and E4, was surprising as these genes have important roles of an array of virus-host interactions. By far, cancer selective Ad research has focused primarily upon the modification of the Ad early genes by the deletion of E1b genes, *E1b-19K* and *E1b-55K*, or the

regulation of E1a gene expression using cancer-selective promoters [40, 53]. These results indicate that the late gene-encoded structural proteins may directly influence oncolytic Ad release and oncolysis. To study these mutations further, each mutation should be introduced into a well characterized Ad vector to understand their impact upon Ad replication and therapy.

During bioselection AdUV regained *E1b*, likely via homologous recombination with the E1 sequences contained within HEK293 cells [52]. UV irradiation has been shown to enhance Ad recombination *in vitro* [54]. These results suggest that *E1b* may benefit Ad cancer therapy, even if *E1b* is not essential for Ads to replicate and lyse cancer cells [38]. *E1b*-deleted Ads are safe, however the mechanism of *E1b*-deleted Ad cancer selectivity has not been fully characterized [23, 55]. Previously, Zhang et. al. showed that Ad E1B-55K can induce the expression of the cell cycle-related genes, cyclin E and CDC25A [35]. The induction of cyclin E by E1B-55K was required for Ads to replicate in normal cells, but not in cancer cells which frequently have deregulated cyclin E expression [56]. The induction of cyclin E following Ad infection stimulates CDK2 phosphorylation at the S612 during Ad infection [56]. Therefore, cyclin E deregulation in cancer cells may be an important target for the cancer selectivity of *E1b-55K* deleted Ads [38]. This study indicates that while *E1b*-deleted Ads are cancer selective they have limited efficacy, implicating the therapeutic potential of *E1b*-wildtype Ads as demonstrated in the literature [57, 58]. Thus, innovative strategies should be explored to develop more effective, cancer selective Ads.

The lethality of the *E1b*-wildtype AdUV was observed upon A549-tumor bearing *in vivo*. Mice were treated with the negative control AdGFP or the experimental AdUV. AdUV treated tumors were significantly smaller than AdGFP treated tumors at day fifty-one (p-value < 0.0001; Fig. 8A). Moreover, all seven AdUV treated mice survived while only two of the eight AdGFP treated mice survived until day 125 (p-value = 0.0005; Fig. 8B). No objective side-effects of AdUV treatment were observed. It is possible that AdUV is safe in mice because human Ad replication is poor in murine cells. These results indicate that AdUV may be therapeutic and safe in immunodeficient murine models.

AdUV had greater efficacy than Adhz60 for the treatment of lung cancer cells *in vitro* and was therapeutically effective *in vivo*. AdUV displayed greater oncolytic efficacy in several cancer cell lines, producing larger plaques than Ad5 (p-value = 0.0248) and Adhz60 (p-value = 0.0002) in A549 cells (Fig. 4B). AdUV was also a more effective autophagy inducer (30.9 fold) than both Ad5 (12.2 fold) and Adhz60 (7.8 fold) in A549 cells (Fig. 6B). It appears that the acquisition of *E1b* and/or mutations to the Ad late genes have increased the oncolytic potential of AdUV. Additional studies may be required to understand how these mutations affect Ad-mediated cancer cell lysis. These mutations should be recombined into an *E1b*-deleted cancer selective Ad vector to determine they are beneficial when incorporated into an *E1b*-deleted Ad background. Selective autophagy inducers will be studied to identify new therapeutic combinations to maximize Ad cancer therapy.

FIGURES

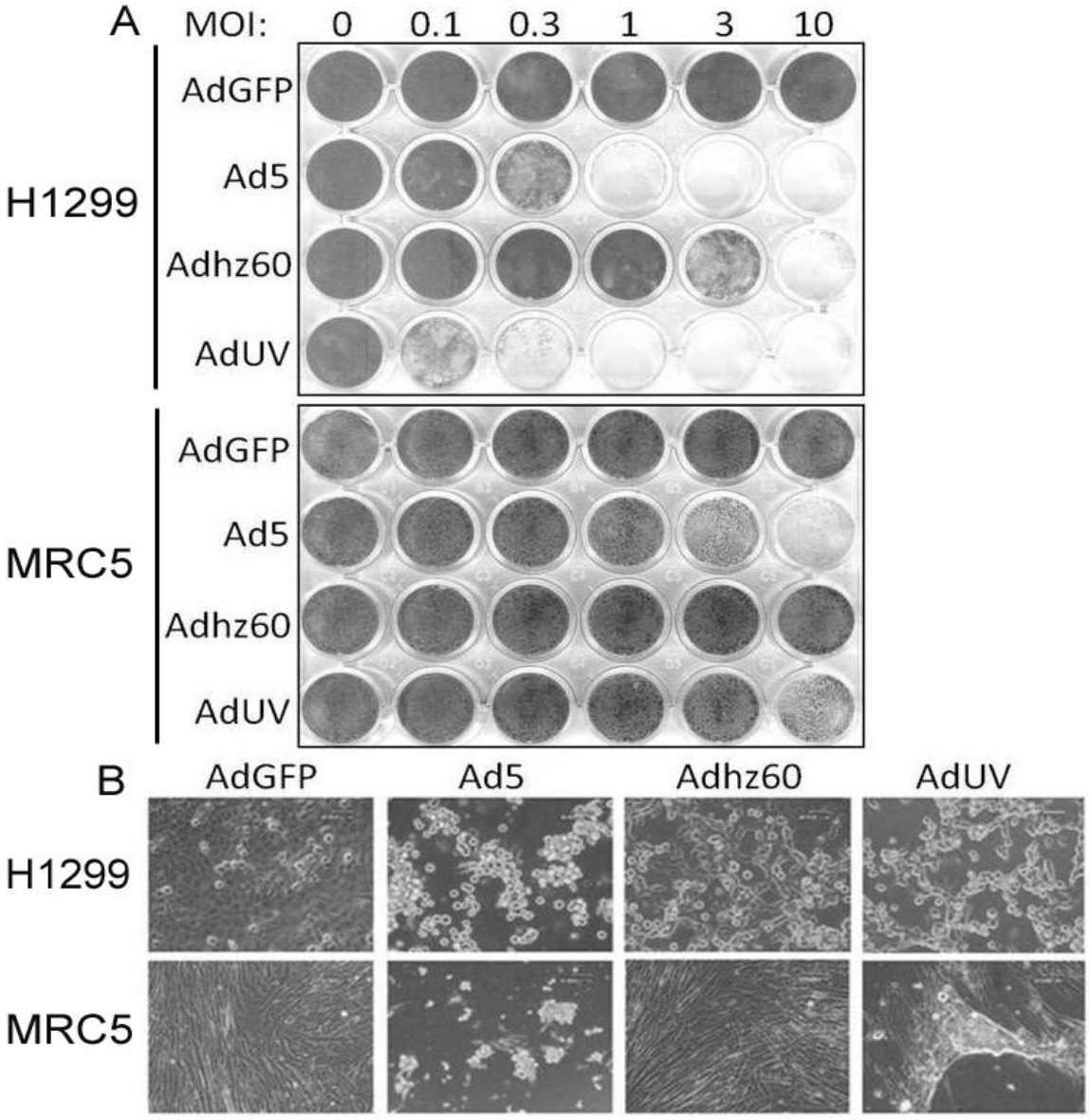

Figure 2. The effect of AdUV upon normal lung and lung cancer cells. A) H1299 lung cancer or MRC5 normal lung cell lines were treated with the indicated MOIs of each adenovirus and stained with crystal violet after five days. B) The Cytopathic effects (CPE) of cells treated at 10 MOI were photographed. H1299 cells were photographed at day 3 post-infection. MRC5 cells were photographed at day 5 post-infection.

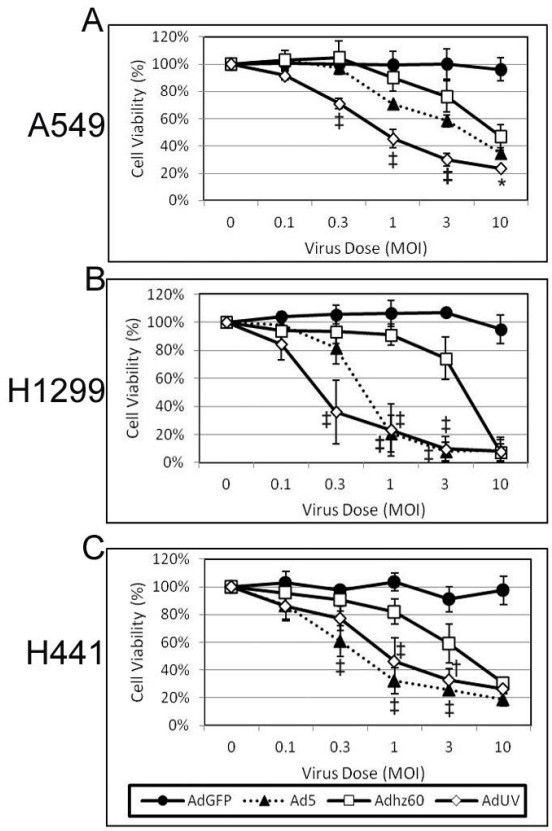

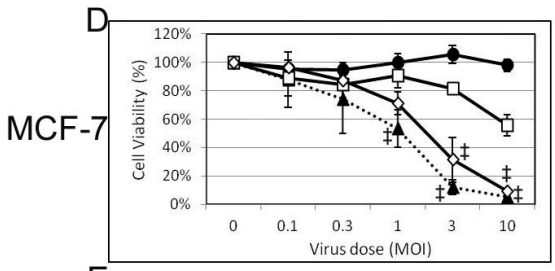

E

	EC50 (MOI)			
Virus	A549	H1299	H441	MCF-7
Ad5	4.11	0.58	0.58	0.84
Adhz60	9.05	4.29	4.29	d.n.e.
AdUV	0.99	1.12	1.12	1.76

F

	ANOVA 1 MOI (p-value)			
Virus	A549	H1299	H441	MCF-7
AdGFP vs. Ad5	n.s.	‡	‡	‡
AdGFP vs. Adhz60	n.s.	n.s.	n.s.	n.s.
AdGFP vs. AdUV	‡	‡	‡	*
Ad5 vs. Adhz60	n.s.	‡	‡	†
Adhz60 vs. AdUV	‡	‡	†	n.s.
Ad5 vs. AdUV	n.s.	n.s.	n.s.	n.s.

Figure 3. AdUV kills multiple cancer cell lines more effectively than Adhz60 *in vitro*. A549, H1299, H441 lung cancer cells and MCF-7 breast cancer cells were treated with AdGFP, Ad5, Adhz60, or AdUV at the indicated MOIs. A-D) Cytotoxicity was determined by crystal violet staining after five days infection. Data was presented as the percent viability of treated cells relative to non-treated cells ± the standard deviation of three independent experiments. E) EC50 values were determined using GraphPad PRISM software. F) Two-way ANOVA with multiple comparisons were conducted between all Ad treatments in each cancer cell line at one MOI. All p-values were adjusted from two-way ANVOA analysis adjusted for post-hoc testing for multiple comparisons corrected by Bonferroni's method. d.n.e. indicates the value does not exist, n.s. indicates a p-value > 0.05, * Indicates a p-value < 0.05, † indicates a p-value < 0.01, ‡ indicates a p-value < 0.001.

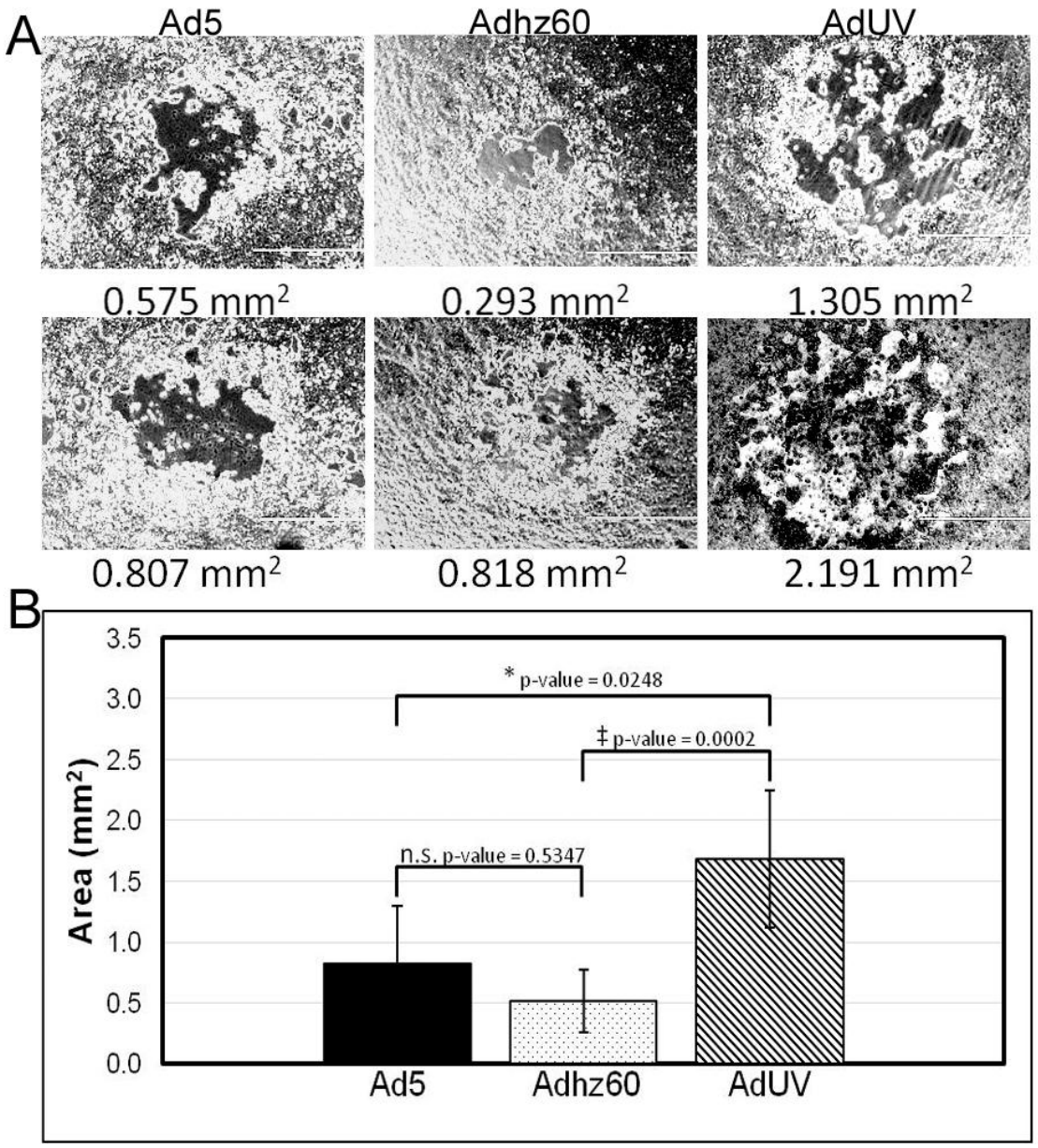

Figure 4. AdUV spread in A549 cell monolayers. A) Two representative plaques of A549 cells treated with Ad5, Adhz60, and AdUV are shown. B) The number of pixels contained within ten representative plaques was determined and divided by the number of pixels per one mm^2 to determine the size of each plaque in millimeters (mm^2). These data were plotted as the average ± the standard deviation of ten plaques each (SD). Statistical significance was assessed using the Wilcoxon rank-sum test. Adjusted p-values were reported for multiple comparisons via Dunn's test. n.s. indicates a p-value > 0.05, † indicates a p-value < 0.01, ‡ indicates a p-value < 0.001.

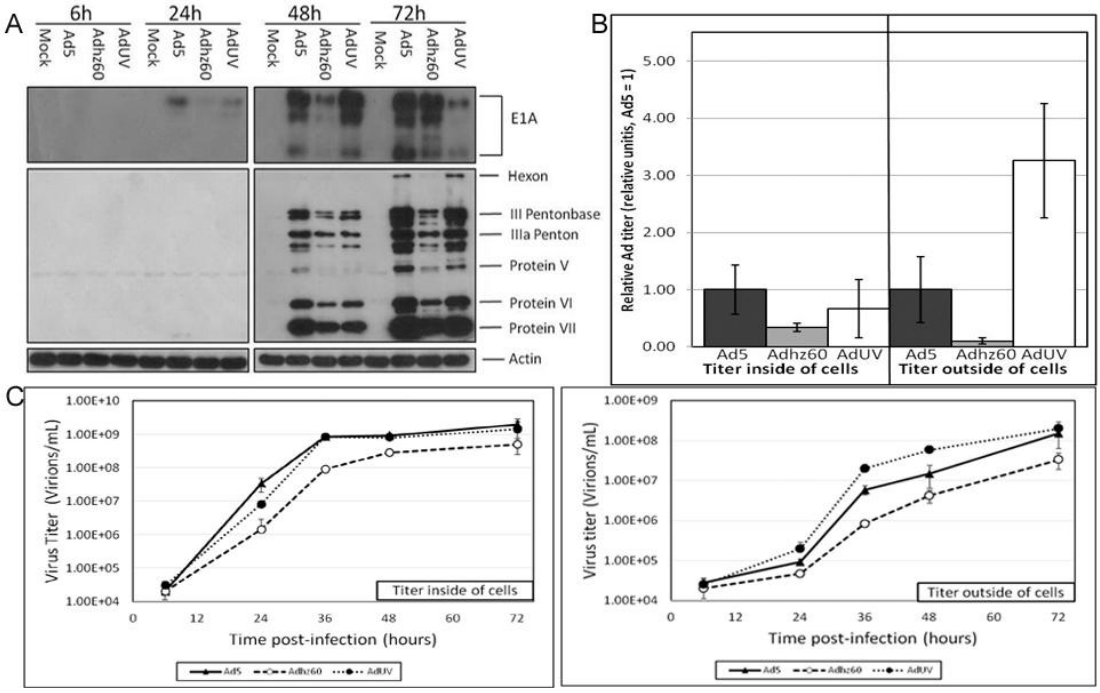

Figure 5. AdUV virus replication in A549 lung cancer cells. A) Ad protein production was observed at different time-points in A549 cells treated with one MOI of Ad5, Adhz60, or AdUV. B) Virus production inside and outside of A549 infected cells at one MOI after 48 hours infection was normalized to the average Ad5 titer. Data is presented relative to Ad5 titer ± the standard deviation (SD) of three independent replicates. C) A549 cells were infected at one MOI and viral production was observed over time inside of and outside of infected A549 cells. Significance was determined via the Wilcoxon rank-sum test. Adjusted p-values were reported for multiple comparisons via Dunn's test. * indicates p-value < 0.05.

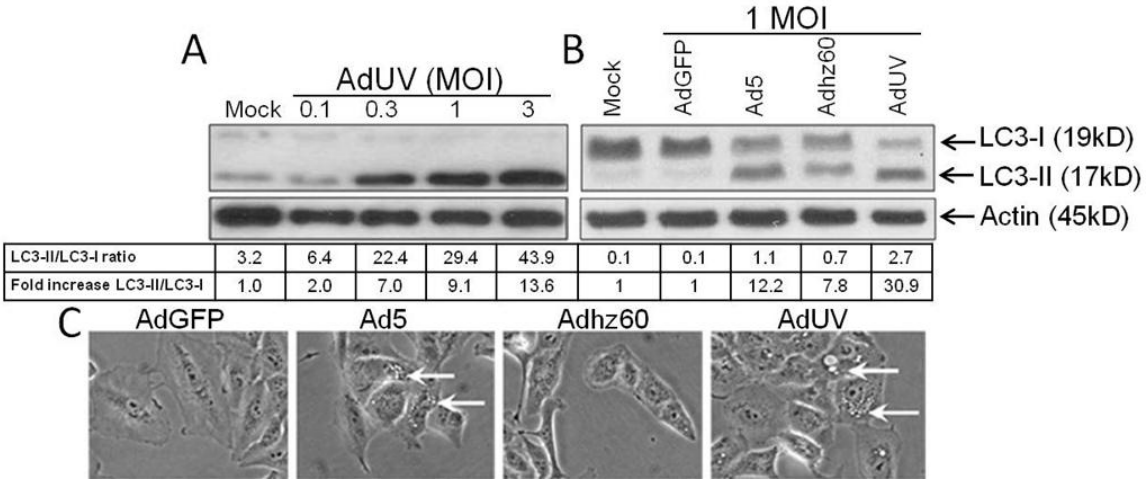

LC3-II/LC3-I ratio	3.2	6.4	22.4	29.4	43.9	0.1	0.1	1.1	0.7	2.7
Fold increase LC3-II/LC3-I	1.0	2.0	7.0	9.1	13.6	1	1	12.2	7.8	30.9

Figure 6. AdUV induces greater autophagy in A549 lung cancer cells. A) A549 cells were infected with increasing MOIs of AdUV for five days. B) A549 cells were treated with one MOI of AdGFP, Ad5, Adhz60 and AdUV for five days. A-B) LC3 expression was observed and the ratio of LC3-II to LC3-I was quantified relative to actin using Gel-pro analyzer 4.0 software. C) Images of A549 cells (400 x total magnification) treated with one MOI of AdGFP, Ad5, Adhz60 and AdUV were shown three days post-infection. Arrowheads indicate cytoplasmic vesicles in Ad treated A549 cells.

A.

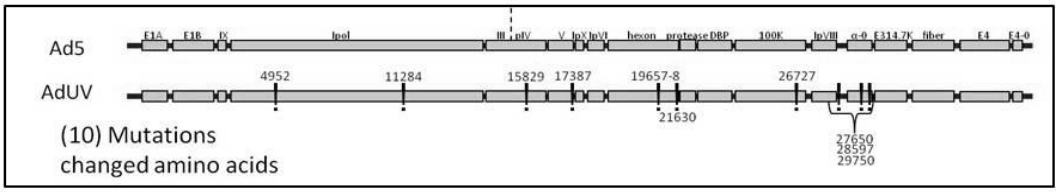

B.

Position	Gene	Mutation	aa Change	Chemical changes
4952	Iva2	G to C	Gly to Ala	Still hydrophobic
11284	Ipol	T to C	Val to Ala	Still hydrophobic
15829	pIII	Non-sense 1 base deletion	Ref: LGIVSPRVLSSRTF UV_1: LA Lost 13 amino acids	Truncation of 13 amino acids
17387	pV	G to C	Gly to Arg	H atom for long basic side-chain
19657 & 8	Hexon	GA to AG Inversion	Ref: Ala Thr UV_1: Ala Ala (replaced neucleophile)	Nucleophile (Thr) replaced by methyl (Ala)
21630	Hexon	G to A	Arg to Glu (basic to acidic)	+ charge to – charge
26727 – 33	33K	Six base deletion	Lost RQ Tandem repeat Ref: HRRQRQRQQQQRPHR UV_1: HRRQRQQQRPHR	Lost two aas, are they important?
27650 – 1	IpVIII	TC to CT Inversion	Ref: Arg Pro UV_1: Arg Ser (lost Pro, added neucleophile)	Proline (structural) lost for a neuclophile (Ser)
28597 to 601	Alpha-0	Six base deletion	Lost Ile and Gly	Lost two aas, are they important?
29750	10.5 kD	T to G	Met to Arg	Hydrophobic (Met) to long basic (Arg)

Figure 7. DNA sequencing of AdUV. A) A genetic map showing the location of mutations detected in AdUV relative to Ad5 wildtype sequences. The boxes indicate the Ad exons. B) Table of AdUV DNA mutations, their location, and changes to their amino acid sequences. The dark gray rows indicate alteration in the amino acid biochemical properties of encoded amino acid sequences. The dose of UV type-C (639 J/m^2) irradiation was produced by a germicidal UV-lamp and measured as described in the materials and methods.

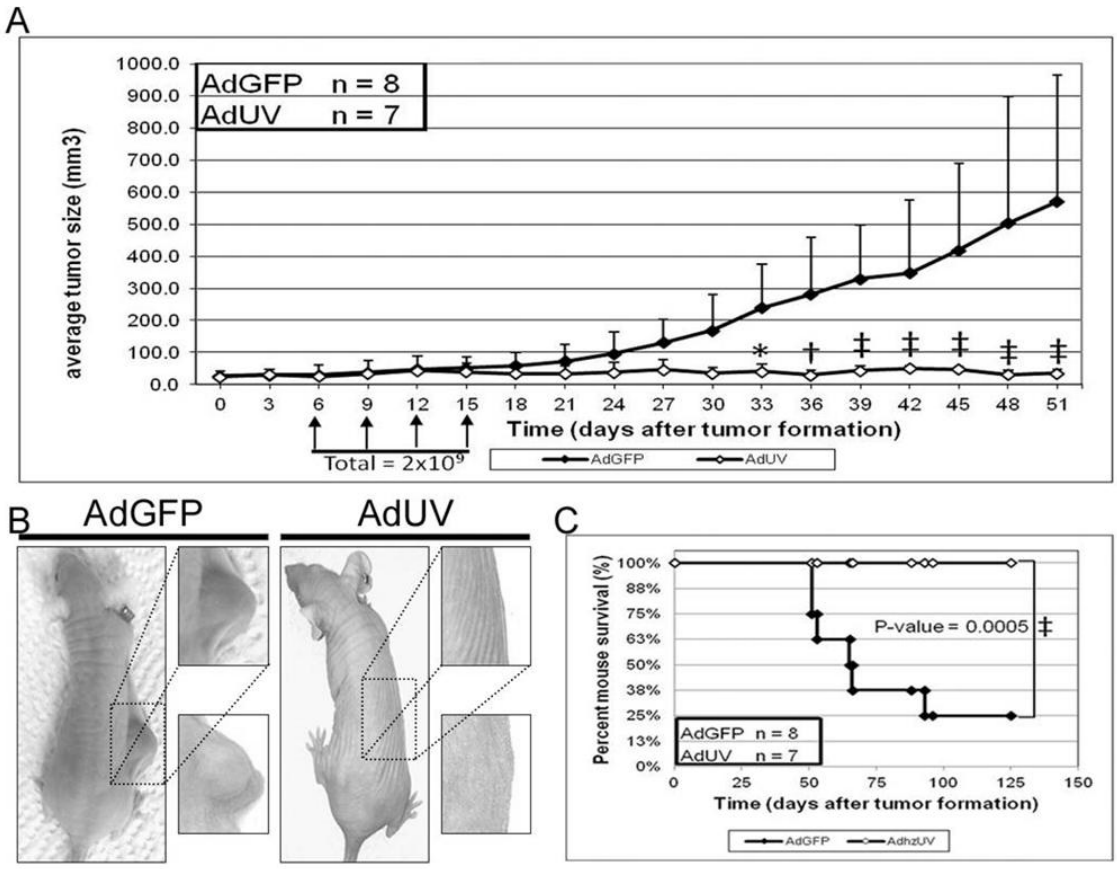

Figure 8. Treatment of xenograft tumors. Subcutaneous A549 tumor xenografts were grown following the subcutaneous injection (SC) of $5x10^6$ A549 cells in the right flank of nu/nu athymic mice. A) Tumors were injected intratumorally (IT) with AdGFP or AdUV once they reached 30 mm^3 in size. Mice were treated by four IT injections from day six until day fifteen for a total dose of $2x10^9$ PFU. B) Representative mice treated with AdGFP and AdUV were photographed at day 51. Boxes indicate the magnified right flank of treated mice. C) Animals were sacrificed once tumors were greater than 1,000 m^3 in size. Differences in tumor growth were assessed by two-way ANOVA with multiple comparisons between the AdGFP and AdUV treatment groups per day. P-values were adjusted via Bonferroni's method. Differences in murine survival were determined using the Kaplan-Meier log-rank sum test. * indicates p-value < 0.05, † indicates p-value < 0.01, ‡ indicates p-value < 0.001.

REFERENCES

1. Tanoue, L.T. and F.C. Detterbeck, *New TNM classification for non-small-cell lung cancer.* Expert Rev Anticancer Ther, 2009. **9**(4): p. 413-23.

2. He, J. and X. Xu, *Thoracoscopic anatomic pulmonary resection.* J Thorac Dis, 2012. **4**(5): p. 520-47.

3. Onaitis, M.W., R.P. Petersen, S.S. Balderson, E. Toloza, W.R. Burfeind, D.H. Harpole, Jr., and T.A. D'Amico, *Thoracoscopic lobectomy is a safe and versatile procedure: experience with 500 consecutive patients.* Ann Surg, 2006. **244**(3): p. 420-5.

4. Zarogoulidis, K., P. Zarogoulidis, K. Darwiche, E. Boutsikou, N. Machairiotis, K. Tsakiridis, N. Katsikogiannis, I. Kougioumtzi, I. Karapantzos, H. Huang, and D. Spyratos, *Treatment of non-small cell lung cancer (NSCLC).* J Thorac Dis, 2013. **5 Suppl 4**: p. S389-96.

5. Wang, E.H., C.D. Corso, C.E. Rutter, H.S. Park, A.B. Chen, A.W. Kim, L.D. Wilson, R.H. Decker, and J.B. Yu, *Postoperative Radiation Therapy Is Associated With Improved Overall Survival in Incompletely Resected Stage II and III Non-Small-Cell Lung Cancer.* J Clin Oncol, 2015.

6. Einhorn, L.H., *First-line chemotherapy for non-small-cell lung cancer: is there a superior regimen based on histology?* J Clin Oncol, 2008. **26**(21): p. 3485-6.

7. Ramalingam, S. and C. Belani, *Systemic chemotherapy for advanced non-small cell lung cancer: recent advances and future directions.* Oncologist, 2008. **13 Suppl 1**: p. 5-13.

8. Schuchert, M.J. and J.D. Luketich, *Solitary sites of metastatic disease in non-small cell lung cancer.* Curr Treat Options Oncol, 2003. **4**(1): p. 65-79.

9. Quint, L.E., S. Tummala, L.J. Brisson, I.R. Francis, A.S. Krupnick, E.A. Kazerooni, M.D. Iannettoni, R.I. Whyte, and M.B. Orringer, *Distribution of distant metastases from newly diagnosed non-small cell lung cancer.* Ann Thorac Surg, 1996. **62**(1): p. 246-50.

10. Schiller, J.H., D. Harrington, C.P. Belani, C. Langer, A. Sandler, J. Krook, J. Zhu, D.H. Johnson, and G. Eastern Cooperative Oncology, *Comparison*

of four chemotherapy regimens for advanced non-small-cell lung cancer. N Engl J Med, 2002. **346**(2): p. 92-8.

11. Heuvers, M.E., J.P. Hegmans, B.H. Stricker, and J.G. Aerts, *Improving lung cancer survival; time to move on.* BMC Pulm Med, 2012. **12**: p. 77.

12. Pollock, J. and E.B. Garon, *Management of small-cell lung cancer: time to move forward.* Oncology (Williston Park), 2010. **24**(11): p. 1043, 1046-7.

13. Parker, J.N., D.F. Bauer, J.J. Cody, and J.M. Markert, *Oncolytic viral therapy of malignant glioma.* Neurotherapeutics, 2009. **6**(3): p. 558-69.

14. Vijayalingam, S., M. Kuppuswamy, T. Subramanian, F.F. Strebeck, C.L. West, M. Varvares, and G. Chinnadurai, *Evaluation of apoptogenic adenovirus type 5 oncolytic vectors in a Syrian hamster head and neck cancer model.* Cancer Gene Ther, 2014. **21**(6): p. 228-37.

15. Nettelbeck, D.M., *Cellular genetic tools to control oncolytic adenoviruses for virotherapy of cancer.* J Mol Med (Berl), 2008. **86**(4): p. 363-77.

16. Fueyo, J., C. Gomez-Manzano, R. Alemany, P.S. Lee, T.J. McDonnell, P. Mitlianga, Y.X. Shi, V.A. Levin, W.K. Yung, and A.P. Kyritsis, *A mutant oncolytic adenovirus targeting the Rb pathway produces anti-glioma effect in vivo.* Oncogene, 2000. **19**(1): p. 2-12.

17. Bischoff, J.R., D.H. Kim, A. Williams, C. Heise, S. Horn, M. Muna, L. Ng, J.A. Nye, A. SampsonJohannes, A. Fattaey, and F. McCormick, *An adenovirus mutant that replicates selectively in p53-deficient human tumor cells.* Science, 1996. **274**(5286): p. 373-376.

18. Zhao, T., X.M. Rao, X. Xie, L. Li, T.C. Thompson, K.M. McMasters, and H.S. Zhou, *Adenovirus with insertion-mutated E1A selectively propagates in liver cancer cells and destroys tumors in vivo.* Cancer Res, 2003. **63**(12): p. 3073-8.

19. Opyrchal, M., I. Aderca, and E. Galanis, *Phase I clinical trial of locoregional administration of the oncolytic adenovirus ONYX-015 in combination with mitomycin-C, doxorubicin, and cisplatin chemotherapy in patients with advanced sarcomas.* Methods Mol Biol, 2009. **542**: p. 705-17.

20. Kirn, D., *Oncolytic virotherapy for cancer with the adenovirus dl1520 (Onyx-015): results of phase I and II trials.* Expert Opin Biol Ther, 2001. **1**(3): p. 525-38.

21. Makower, D., A. Rozenblit, H. Kaufman, M. Edelman, M.E. Lane, J. Zwiebel, H. Haynes, and S. Wadler, *Phase II clinical trial of intralesional*

administration of the oncolytic adenovirus ONYX-015 in patients with hepatobiliary tumors with correlative p53 studies. Clin Cancer Res, 2003. **9**(2): p. 693-702.

22. Heise, C., A. Sampson-Johannes, A. Williams, F. McCormick, D.D. Von Hoff, and D.H. Kirn, *ONYX-015, an E1B gene-attenuated adenovirus, causes tumor-specific cytolysis and antitumoral efficacy that can be augmented by standard chemotherapeutic agents.* Nat Med, 1997. **3**(6): p. 639-45.

23. Yu, W. and H. Fang, *Clinical trials with oncolytic adenovirus in China.* Curr Cancer Drug Targets, 2007. **7**(2): p. 141-8.

24. Xia, Z.J., J.H. Chang, L. Zhang, W.Q. Jiang, Z.Z. Guan, J.W. Liu, Y. Zhang, X.H. Hu, G.H. Wu, H.Q. Wang, Z.C. Chen, J.C. Chen, Q.H. Zhou, J.W. Lu, Q.X. Fan, J.J. Huang, and X. Zheng, *[Phase III randomized clinical trial of intratumoral injection of E1B gene-deleted adenovirus (H101) combined with cisplatin-based chemotherapy in treating squamous cell cancer of head and neck or esophagus].* Ai Zheng, 2004. **23**(12): p. 1666-70.

25. Waszak, P., M.L. Franco-Montoya, M.P. Jacob, I. Deprez, M. Levame, C. Lafuma, A. Harf, and C. Delacourt, *Effect of intratracheal adenoviral vector administration on lung development in newborn rats.* Hum Gene Ther, 2002. **13**(15): p. 1873-85.

26. You, L., C.T. Yang, and D.M. Jablons, *ONYX-015 works synergistically with chemotherapy in lung cancer cell lines and primary cultures freshly made from lung cancer patients.* Cancer Res, 2000. **60**(4): p. 1009-13.

27. Nemunaitis, J., C. Cunningham, A. Buchanan, A. Blackburn, G. Edelman, P. Maples, G. Netto, A. Tong, B. Randlev, S. Olson, and D. Kirn, *Intravenous infusion of a replication-selective adenovirus (ONYX-015) in cancer patients: safety, feasibility and biological activity.* Gene Ther, 2001. **8**(10): p. 746-59.

28. Cheng, P.H., S. Lian, R. Zhao, X.M. Rao, K.M. McMasters, and H.S. Zhou, *Combination of autophagy inducer rapamycin and oncolytic adenovirus improves antitumor effect in cancer cells.* Virol J, 2013. **10**: p. 293.

29. Chan, L., P.H. Cheng, X.M. Rao, K.M. McMasters, and H.S. Zhou, *Indole-3-carbinol (I3C) increases apoptosis, represses growth of cancer cells, and enhances adenovirus-mediated oncolysis.* Cancer Biol Ther, 2014. **15**(9).

30. Lu, W., S. Zheng, X.F. Li, J.J. Huang, X. Zheng, and Z. Li, *Intra-tumor injection of H101, a recombinant adenovirus, in combination with chemotherapy in patients with advanced cancers: a pilot phase II clinical trial.* World J Gastroenterol, 2004. **10**(24): p. 3634-8.

31. Xu, R.H., Z.Y. Yuan, Z.Z. Guan, Y. Cao, H.Q. Wang, X.H. Hu, J.F. Feng, Y. Zhang, F. Li, Z.T. Chen, J.J. Wang, J.J. Huang, Q.H. Zhou, and S.T. Song, *[Phase II clinical study of intratumoral H101, an E1B deleted adenovirus, in combination with chemotherapy in patients with cancer].* Ai Zheng, 2003. **22**(12): p. 1307-10.

32. Yan, W., G. Kitzes, F. Dormishian, L. Hawkins, A. Sampson-Johannes, J. Watanabe, J. Holt, V. Lee, T. Dubensky, A. Fattaey, T. Hermiston, A. Balmain, and Y. Shen, *Developing novel oncolytic adenoviruses through bioselection.* J Virol, 2003. **77**(4): p. 2640-50.

33. Gros, A., J. Martinez-Quintanilla, C. Puig, S. Guedan, D.G. Mollevi, R. Alemany, and M. Cascallo, *Bioselection of a gain of function mutation that enhances adenovirus 5 release and improves its antitumoral potency.* Cancer Res, 2008. **68**(21): p. 8928-37.

34. Beier, R., T. Hermiston, and D. Mumberg, *Isolation of more potent oncolytic paramyxovirus by bioselection.* Gene Ther, 2013. **20**(1): p. 102-11.

35. Rao, X.M., X. Zheng, S. Waigel, W. Zacharias, K.M. McMasters, and H.S. Zhou, *Gene expression profiles of normal human lung cells affected by adenoviral E1B.* Virology, 2006. **350**(2): p. 418-28.

36. Rao, X.M., M.T. Tseng, X. Zheng, Y. Dong, A. Jamshidi-Parsian, T.C. Thompson, M.K. Brenner, K.M. McMasters, and H.S. Zhou, *E1A-induced apoptosis does not prevent replication of adenoviruses with deletion of E1b in majority of infected cancer cells.* Cancer Gene Ther, 2004. **11**(9): p. 585-93.

37. *UV Lamps for Gemicidal Applications General Electric Company.*; Available from: Available at :www.gelighting.com. Accessed Febuary 2, 2015.

38. Zheng, X., X.M. Rao, J.G. Gomez-Gutierrez, H. Hao, K.M. McMasters, and H.S. Zhou, *Adenovirus E1B55K region is required to enhance cyclin E expression for efficient viral DNA replication.* J Virol, 2008. **82**(7): p. 3415-27.

39. Sandig, V., R. Youil, A.J. Bett, L.L. Franlin, M. Oshima, D. Maione, F. Wang, M.L. Metzker, R. Savino, and C.T. Caskey, *Optimization of the*

helper-dependent adenovirus system for production and potency in vivo. Proc Natl Acad Sci U S A, 2000. **97**(3): p. 1002-7.

40. Cheng, P.H., X.M. Rao, X. Duan, X.F. Li, M.E. Egger, K.M. McMasters, and H.S. Zhou, *Virotherapy targeting cyclin E overexpression in tumors with adenovirus-enhanced cancer-selective promoter.* J Mol Med (Berl), 2014.

41. Ishiyama, M., H. Tominaga, M. Shiga, K. Sasamoto, Y. Ohkura, and K. Ueno, *A combined assay of cell viability and in vitro cytotoxicity with a highly water-soluble tetrazolium salt, neutral red and crystal violet.* Biol Pharm Bull, 1996. **19**(11): p. 1518-20.

42. Kondo, Y., T. Kanzawa, R. Sawaya, and S. Kondo, *The role of autophagy in cancer development and response to therapy.* Nat Rev Cancer, 2005. **5**(9): p. 726-34.

43. Kim, H.J., S. Lee, and J.U. Jung, *When autophagy meets viruses: a double-edged sword with functions in defense and offense.* Semin Immunopathol, 2010. **32**(4): p. 323-41.

44. Chen, Y., M.B. Azad, and S.B. Gibson, *Methods for detecting autophagy and determining autophagy-induced cell death.* Can J Physiol Pharmacol, 2010. **88**(3): p. 285-95.

45. Barth, S., D. Glick, and K.F. Macleod, *Autophagy: assays and artifacts.* J Pathol, 2010. **221**(2): p. 117-24.

46. Kabeya, Y., N. Mizushima, T. Ueno, A. Yamamoto, T. Kirisako, T. Noda, E. Kominami, Y. Ohsumi, and T. Yoshimori, *LC3, a mammalian homologue of yeast Apg8p, is localized in autophagosome membranes after processing.* EMBO J, 2000. **19**(21): p. 5720-8.

47. *Ion torrent* Available from: https://ionreporter.lifetechnologies.com/ir/.

48. Davison, A.J., M. Benko, and B. Harrach, *Genetic content and evolution of adenoviruses.* J Gen Virol, 2003. **84**(Pt 11): p. 2895-908.

49. Bergstrom Lind, S., K.A. Artemenko, L. Elfineh, Y. Zhao, J. Bergquist, and U. Pettersson, *Post translational modifications in adenovirus type 2.* Virology, 2013. **447**(1-2): p. 104-11.

50. Zhang, W., J.A. Low, J.B. Christensen, and M.J. Imperiale, *Role for the adenovirus IVa2 protein in packaging of viral DNA.* J Virol, 2001. **75**(21): p. 10446-54.

51. Matthews, D.A. and W.C. Russell, *Adenovirus core protein V interacts with p32--a protein which is associated with both the mitochondria and the nucleus.* J Gen Virol, 1998. **79 (Pt 7)**: p. 1677-85.

52. Kuwata, T., T. Oda, S. Sekiya, and N. Morinaga, *Characteristics of a human cell line successively transformed by Rous sarcoma virus and simian virus 40.* J Natl Cancer Inst, 1976. **56**(5): p. 919-26.

53. Nettelbeck, D.M., V. Jerome, and R. Muller, *Gene therapy: designer promoters for tumour targeting.* Trends Genet, 2000. **16**(4): p. 174-81.

54. Rainbow, A.J. and J.E. Castillo, *Homologous recombination of adenovirus DNA in mammalian cells: enhanced recombination following UV-irradiation of the virus.* Mutat Res, 1992. **274**(3): p. 201-10.

55. Alemany, R., *Cancer selective adenoviruses.* Mol Aspects Med, 2007. **28**(1): p. 42-58.

56. Cheng, P.H., X.M. Rao, K.M. McMasters, and H.S. Zhou, *Molecular basis for viral selective replication in cancer cells: activation of CDK2 by adenovirus-induced cyclin E.* PLoS One, 2013. **8**(2): p. e57340.

57. Klein, S.R., S. Piya, Z. Lu, Y. Xia, M.M. Alonso, E.J. White, J. Wei, C. Gomez-Manzano, H. Jiang, and J. Fueyo, *C-Jun N-terminal kinases are required for oncolytic adenovirus-mediated autophagy.* Oncogene, 2015.

58. Jiang, H., C. Gomez-Manzano, R. Alemany, D. Medrano, M. Alonso, B.N. Bekele, E. Lin, C.C. Conrad, W.K. Yung, and J. Fueyo, *Comparative effect of oncolytic adenoviruses with E1A-55 kDa or E1B-55 kDa deletions in malignant gliomas.* Neoplasia, 2005. **7**(1): p. 48-56.

APPENDIX

List of Abbreviations

Ad	Adenovirus
Ad2	Adenovirus serotype 2
Ad5	Adenovirus serotype 5
Ads	Adenoviruses
AEBSF	4-(2-aminoethyl)-benzenesulfonyl fluoride
ANOVA	Analysis of Variance
Atg	Autophagy related
CFDA	China Food and Drug Administration
ddH_20	Double Distilled Water
DMEM	Dulbecco's Modified Eagle Medium
E1A	Early gene 1 A
E1B	Early gene 1 B
ECL	Enhanced Chemiluminescence
FBS	Fetal Bovine Serum
GFP	Green Fluorescent Protien
HRP	Horse Radish Peroxidase
Ig	immunoglobin

IGV	Integrated Genomics Viewer
IT	Intratumoral injection
IV	Intravenous injection
LC3	Light Chain 3
MOI	Multiplicity of Infection
OD	Opitical Density or absorbance
PBS	Phosphate Buffered Saline
PFU	Plaque Forming Units
PI	Protease Inhibitor
RCF	Relative Centrifugal Force
RIPA	Radioimmunoprecipitation Assay Buffer
RPM	Revolutions Per Minute
RPMI	Roswell Park Memorial Institute
SC	Subcutaneous injection
SDS	Sodium Dodecyl Sulfate
SEER	Surveillance Epidemiology and End Results
TBST	Tris-Buffered saline with Tween 20
TNM	Tumor Nodes Metastatsis
Wt	Wildtype

CURRICULUM VITAE

Stephen Wechman
Curriculum Vitae January 2014
505 South Hancock CTR Building, room# 452G
Louisville, KY, 40202
Phone #: (502) 316-0370
Fax #: (502) 852-3661
slwech01@louisville.edu

EDUCATION

2007 - 2011 B.S. in Biology, Georgetown College, Georgetown, KY
2011 - M.S. in Pharmacology and Toxicology, University of Louisville, Louisville, KY
2011 - Ph.D. in Pharmacology and Toxicology, University of Louisville, Louisville, KY

ACADEMIC APPOINTMENTS

2013 - 2014 Teaching Assistant
Department of Pharmacology and Toxicology
University of Louisville
Louisville, KY

2011 - Graduate Student Research Fellow
Department of Pharmacology and Toxicology
University of Louisville
Louisville, KY

PROFESSIONAL MEMBERSHIPS AND ACTIVITIES

2014 - American Association for Cancer Research
2012 - Kentucky Academy of Science
2011 - 2012 Society of Toxicology

HONORS AND AWARDS

2014 2nd place Kentucky Academy of Sciences, Graduate Research presentation, University of Kentucky
2014 2nd place Condict Moore research prize, James Graham Brown Cancer Center Retreat, University of Louisville
2014 2nd place Research Louisville!, Masters Candidate, poster competition, University of Louisville
2013 1st place Kentucky Academy of Science, Graduate Research, Morehead University
2013 3rd place Research Louisville!, Masters Candidate, poster competition, University of Louisville
2013 Featured in Georgetown College, “College to Career” publication, Georgetown College
2011 Graduate Fellowship from the Integrated Programs in Biomedical Sciences (IPIBS), University of Louisville

2011 Top 15% worldwide, Mathematical Competition in Modeling, Georgetown College
2010 Georgetown College Program for the Accelerated Learning in Sciences fellowship
2003 Member, Honorable Order of Kentucky Colonels honor society
2003 Eagle Scout award

TEACHING ACTIVITIES
University of Louisville (2013-present; all courses are team taught)

2014

- 8/29 Patient SIM session ***"Pharmacology SIM Session on Autonomics"*** Medical school students
- 4/12 Instructor, BIOL-395-01 **"*Cancer Chemotherapy: part 2 chemotherapy drugs*"** Undergraduates
- 4/10 Instructor, BIOL-395-01 **"*Cancer Chemotherapy: part 1 cancer and the cell cycle*"** Undergraduates
- 3/18 Instructor, BIOL-395-01 ***"Hormone Pharmacology: Androgens and Estrogens"*** Undergraduate Students

2013

- 11/18 Instructor, DHED-402-01 **"*Dental Pharmacology: Cancer Chemotherapy Lecture"*** Dental Hygiene
- 4/16 Instructor, BIOL-395-01 **"*Cancer Chemotherapy: part 2 chemotherapy drugs*"** Undergraduates
- 4/11 Instructor, BIOL-395-01 **"*Cancer Chemotherapy: part 1 cancer and the cell cycle*"** Undergraduates
- 9/9 Patient SIM session ***"Pharmacology SIM Session on Autonomics"*** Medical school students
- Spring Teaching assistant, Supervised by Dr. Steven Myers for BIOL-395 **Introduction to pharmacology**

GRANTS AND CONTRACTS

Past

Title: Georgetown College Program for accelerated learning in the sciences (GC-PALS) Fellowship
Role in Project: Undergraduate Researcher, Georgetown College
Principal Investigator: Mark Christensen (Georgetown College)
Funding Agency: Howard Hughes Medical Institute
Project Period: May 3, 2010 to August 6, 2010
Project Award: $4,000 (total)

Title: Integrated Programs in Biomedical Sciences (IPIBS) Fellowship
Role in Project: Graduate Student Researcher, University of Louisville
Principal Investigator: Thomas Geoghegan (University of Louisville)
Funding Agency: University of Louisville
Project Period: August 1, 2011 to June 1, 2013
Project Award: $40,326 (total)

ORAL PRESENTATIONS

Local/Regional Meetings

1. **Stephen Wechman,** X. M. Rao, H. S. Zhou, Kelly McMasters. *AdUV has greater potency, replication, and spread within lung cancer cells.* University of Louisville. Kentucky Academy of Science at Moorhead University, Moorhead, Kentucky

2. **Wechman, S.L.,** Rao X.M., McMasters K.M., Heshan, Z. 2014, *Next generation oncolytic therapy is highly active against lung cancer.* OVSOT Summer Meeting at the University of Louisville, Louisville, Kentucky.

3. **Wechman, S.L,** Rao X. M., Gao H., McMasters K. M., Zhou, H., 2014. *Viability of losartan and other anti-fibrotics in combination with oncolytic adenovirus therapy.* Kentucky Academy of Science at the University of Kentucky, Lexington, Kentucky.

POSTERS

Local/Regional Meetings

1. **Wechman, S.L.,** and Garcia-Ramos, G. 2011. *Comparisons of inhibitory techniques against HIV-1 using recombinant viruses.* Abstract for poster presentation, Kentucky Academy of Sciences Cellular and Molecular Biology section, Murray, KY.

2. **Wechman, S.L.,** Rao, X.M., Cheng, P.H., Hao, H., Gomez-Gutierrez, J., McMasters, K.M., Heshan, Z. 2012. *Insights from novel UV mutant oncolytic E1b-deleted adenoviruses for cancer gene therapy.* Abstract for poster presentation, Research! Louisville, Louisville, KY.

3. **Wechman, S.L.,** Rao, X.M., McMasters, K.M., Heshan, Z. 2013. *AdUV has greater potency, replication, and spread within lung cancer cells*. Abstract for poster presentation, Research! Louisville, Louisville, KY.

4. **Wechman, S.L.,** Rao, X.M., McMasters, K.M., Heshan, Z. 2013. *AdUV has greater potency, replication, and spread within lung cancer cells*. Abstract for poster presentation, Brown Cancer Center Retreat, Louisville, Louisville, KY.

5. **Wechman, S.L.**, Rao, X.M., McMasters, K.M., Heshan, Z. 2014. AdUV has greater potency, replication, and spread within lung cancer cells. Abstract for poster presentation. Research Louisville, University of Louisville, Louisville, KY.

6. Gao, H. Rao. X. M., **Wechman. S. L.,** McMasters, K.M., Heshan, Z. 2014. Viability of losartan and other anti-fibrotics in combination with oncolytic adenovirus therapy. Abstract for poster presentation. Research Louisville, University of Louisville, Louisville, KY.

7. **Wechman, S.L.**, Rao, X.M., McMasters, K.M., Heshan, Z. 2014. AdUV has greater potency, replication, and spread within lung cancer cells. Abstract for poster presentation. James Graham Brown Cancer Center Retreat, University of Louisville, Louisville, KY.

8. Gao, H. Rao. X. M., **Wechman. S. L.,** McMasters, K.M., Heshan, Z. 2014. Viability of losartan and other anti-fibrotics in combination with oncolytic adenovirus therapy. Abstract for poster presentation. James Graham Brown Cancer Center Retreat, University of Louisville, Louisville, KY.

Manuscripts in progress

1. **Stephen L. Wechman**, Pei-Hsin Cheng, Kelly M. McMasters, and H. Sam Zhou. *Insights into optimized oncolytic adenovirus design*.

2. Pei-Hsin Cheng, **Stephen L. Wechman**, Kelly M. McMasters, and H. Sam Zhou. *Molecular mechanisms of oncolytic therapy with adenoviruses.*

Submitted manuscripts

1. Pei-Hsin Cheng, Xiao-Mei Rao, **Stephen L. Wechman**, Kelly M. McMasters, and H. Sam Zhou. *Murine Lung Cancer Model Presenting Potential Clinical Challenges for Oncolytic Adenoviral Therapies. Submitted to Cancer Biology & Therapy*.

PANEL DISCUSSIONS

1. Interested in graduate school: Panel discussion for current Georgetown College Students. Georgetown College, Georgetown, KY, September 27, 2012

COMMUNITY SERVICE

MEMBER, Newtown Christian Church, Choir (2005-2011)
MEMBER, Deacon, Newtown Christian Church (2010-2011)
CHAIR, Head Deacon, Newtown Christian Church (2010)